Calmodulin Inhibitors from *Aspergillus stromatoides*

by **Martín González-Andrade**[a][b][1], **Paulina Del Valle**[a][1], **Martha L. Macías-Rubalcava**[c], **Alejandro Sosa-Peinado**[d], **María Del Carmen González**[e], and **Rachel Mata***[a]

[a]) Facultad de Química, Universidad Nacional Autónoma de México, México DF 04510, México (phone: +525-55-622-5289; e-mail: rachel@unam.mx)

[b]) Instituto Nacional de Medicina Genómica (INMEGEN), Secretaría de Salud, México City DF 14610, México

[c]) Instituto de Química, Universidad Nacional Autónoma de México, México DF 04510, México

[d]) Facultad de Medicina, Universidad Nacional Autónoma de México, México DF 04510, México

[e]) Instituto de Biología, Universidad Nacional Autónoma de México, México DF 04510, México

An organic extract was prepared from the culture medium and mycelia of the marine fungus *Aspergillus stromatoides* RAPER & FENNELL. The extract was fractionated *via* column chromatography, and the resulting fractions were tested for their abilities to quench the fluorescence of the calmodulin (CaM) biosensor *h*CaM M124C-*mBBr*. From the active fraction, emodin (**1**) and ω-hydroxyemodin (**2**) were isolated as CaM inhibitors. Anthraquinones **1** and **2** quenched the fluorescence of the *h*CaM M124C-*mBBr* biosensor in a concentration-dependent manner with K_d values of 0.33 and 0.76 μM, respectively. The results were compared with those of chlorpromazine (CPZ), a classical inhibitor of CaM, with a K_d value of 1.25 μM. Docking analysis revealed that **1** and **2** bind to the same pocket of CPZ. The CaM inhibitor properties of **1** and **2** were correlated with some of their reported biological properties. Citrinin (**3**), methyl 8-hydroxy-6-methyl-9-oxo-9*H*-xanthene-1-carboxylate (**4**), and coniochaetone A (**5**) were also isolated in the present study. The X-ray structure of **5** is reported for the first time.

Introduction. – Calmodulin (CaM) is the major ubiquitous Ca^{2+}-binding protein of all eukaryotes fundamental to the regulation of several cellular events. Structurally, CaM is an acidic small protein composed of *ca.* 148 amino acids organized in two distinct N- and C-terminal globular domains. CaM interacts with, and activates, a surprisingly diverse set of target enzymes such as nitric oxide synthases, adenylate cyclases, phosphodiesterases, several kinases, calcium-ATPase pumps, ion channels, phosphatases, as well as cytoskeletal structural proteins. Consequently, CaM is involved in a variety of physiological and pathophysiological functions related with cancer, including the immune response, as well as cell growth, differentiation, and proliferation, among others [1–3]. Thus, CaM is a relevant molecular target for developing new drugs for the treatment of cancer, a leading cause of death worldwide. Some evidences suggest that CaM inhibition contributes to sensitizing cancer cells to antineoplasic drugs such as cisplatin and bleomycin [4], and to avoid the proliferation of prostate [5] and breast [6] cancer cells.

[1]) These authors contributed equally to this work.

Fungi, in particular marine-derived [7] and endophytic fungi, have become an attractive source of pharmacologically active metabolites including CaM inhibitors useful for the development of new drugs and research tools. Therefore, continuing with our search of natural CaM inhibitors [8], the present investigation was undertaken to discover novel CaM-inhibiting agents from the marine-derived fungus *Aspergillus stromatoides* RAPER & FENNELL (Ascomycota, Eurotiales). This species has not been subject of previous investigations; nevertheless, the genus *Aspergillus* is an important source of bioactive molecules with antiviral, antimicrobial, cytotoxic, and hypocholesterolemic actions, *inter alia* [9].

Results and Discussion. – *Isolation and Characterization of Compounds* **1**–**5**. Bioassay-guided fractionation of an extract prepared from the mycelium and culture medium of *A. stromatoides* led to the isolation and characterization of two compounds from the active fraction (see *Exper. Part*), namely emodin (**1**) and ω-hydroxyemodin (**2**), known also as citreorosein. In addition, citrinin (**3**), methyl 8-hydroxy-6-methyl-9-oxo-9*H*-xanthene-1-carboxylate (**4**), and coniochaetone A (**5**) were identified. The spectroscopic and spectrometric properties of **1**–**5** were identical to those previously reported ([10–14], resp.). The presence of anthraquinones and citrinin in the genus *Aspergillus* [9] and other fungal genera [12][13] is well-documented; however, the occurrence of compound **5** is more limited; so far, it has been isolated only in two coprophilous species of the genus *Coniochaeta* [14].

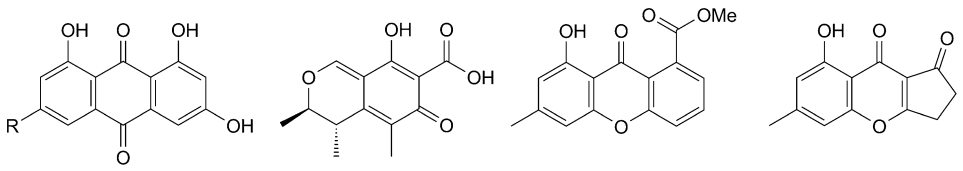

In the present study, the structure of compound **5** was unambiguously established by an X-ray analysis. Suitable crystals of **5** were obtained from CH_2Cl_2. The structure was solved by means of X-ray data collected with MoK_α radiation (*Fig. 1*). The crystallographic data of **5** are compiled in *Table 1*, and bond lengths and angles in *Table 2*. The compound exhibits one intramolecular H-bond with an O(3)–H(3)$\cdots$O(2) angle of 154(3)°, and with O(3)–H(3), H(3)$\cdots$O(2), and O(3)$\cdots$O(2) distances of 0.857(10), 1.796 (17), and 2.595(3) Å, respectively. The molecule is almost planar, the phenyl ring and the γ-pyrone being essentially planar, while the five-membered ring adopts a pseudo-envelope conformation.

Affinity and Docking Studies of Compounds **1** *and* **2** *on* $(Ca^{+2})_4$-h*CaM Complex*. The affinity of compounds **1** and **2** with $(Ca^{+2})_4$-*h*CaM complex in solution was determined using the fluorescent biosensor (*h*CaM M124C-*mBBr*) [15]. The results showed that only the non-heterocyclic compounds **1** and **2** quenched the fluorescence of the biosensor in a concentration-dependent manner (*Table 3* and *Fig. 2*, *a*–*c*). According to the experimental dissociation constants (K_d), the affinity of compounds **1** (K_d = 0.33 μM) and **2** (K_d = 0.76 μM) to the $(Ca^{+2})_4$-*h*CaM complex was slightly better

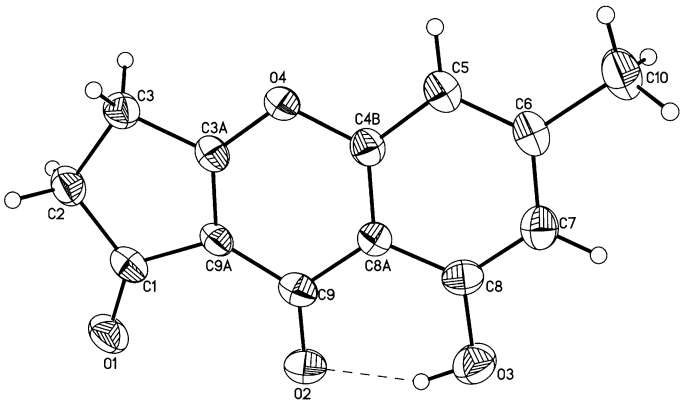

Fig. 1. *ORTEP View of compound* **5**, *showing the atom labeling*

Table 1. *Crystal Data and Structure Refinement for Coniochaetone A* (**5**)

Empirical formula	$C_{13}H_{10}O_4$	Absorption coefficient	0.111 mm^{-1}
Formula weight	230.21	$F(000)$	480
Temp.	298(2) K	Crystal size	$0.30 \times 0.09 \times 0.04$ mm
Wavelength	0.71073 Å	θ Range for data collection	1.99 to 25.41°
Crystal system	Triclinic	Index ranges	$-7 \leq h \leq 7$, $-9 \leq k \leq 9$,
Space group	$P1$		$-25 \leq l \leq 25$
Unit-cell dimensions	$a = 6.2038(17)$ Å	Reflections collected	8544
	$b = 8.108(2)$ Å	Independent reflections	3779 (R(int) = 0.0499)
	$c = 20.947(6)$ Å	Completeness to $\theta = 25.41°$	99.4%
	$\alpha = 79.357(4)$	Refinement method	Full-matrix least-squares on F^2
	$\beta = 84.180(4)°$	Data/restraints/parameters	3779/2/315
	$\gamma = 86.523(5)°$	Goodness-of-fit on F^2	0.859
V	1029.2(5) $Å^3$	Final R indices [$I > 2\sigma(I)$]	$R_1 = 0.0497$, $wR_2 = 0.0922$
Z	4	R Indices (all data)	$R_1 = 0.1384$, $wR_2 = 0.1076$
Density (calc.)	1.486 Mg/m^3	Largest diff. peak and hole	0.340 and -0.151 e $Å^{-3}$

than that of chlorpromazine (CPZ, $K_d = 1.25$ μM); in each case, the binding stoichiometry was 4:1, 3:1, and 7:1, respectively. This set of results also revealed that, among the two anthraquinones, **1** exhibited a slightly higher affinity for the $(Ca^{+2})_4$-*h*CaM complex; this effect could be related with the higher hydrophobic character of **1** due to the presence of a Me group at C(6) [16–18]. Compounds **3**–**5** were also tested, but none of them quenched the fluorescence of the biosensor; as an example, the result for citrinin (**3**) is shown in *Fig. 2*, *d*.

CaM possesses four well-defined interaction regions rich in hydrophobic amino acids [19] where most inhibitors interact. Thus, to obtain a plausible molecular model for the interaction of **1** and **2** with $(Ca^{+2})_4$-*h*CaM, a docking study was conducted with the programs AutoDock 4.0.2 [20][21], AutoDockTools 1.5.4, and LigPlot v.4.0 [22]. AutoDock provides a theoretical inhibition (affinity) constant from docking energy according to the following equation: $K_i = \exp(\Delta G \times 1000)/RT)$, where ΔG = docking energy; $R = 1.98719$ cal K^{-1} mol^{-1}, $T = 298.15$ K, and K_i = inhibition (affinity) constant.

Table 2. *Bond Lengths* [Å] *and Angles* [°] *of* **5** (see *Fig. 1*)

O(1)–C(1)	1.221(3)	C(1)–C(2)–C(3)	106.6(3)
O(2)–C(9)	1.243(3)	C(3A)–C(3)–C(2)	102.0(2)
O(3)–C(8)	1.355(3)	O(4)–C(3A)–C(9A)	125.8(3)
O(3)–H(3)	0.857(10)	O(4)–C(3A)–C(3)	118.4(3)
O(4)–C(3A)	1.331(3)	C(9A)–C(3A)–C(3)	115.8(3)
O(4)–C(4B)	1.394(3)	C(5)–C(4B)–O(4)	115.7(3)
C(1)–C(9A)	1.468(4)	C(5)–C(4B)–C(8A)	124.3(3)
C(1)–C(2)	1.509(4)	O(4)–C(4B)–C(8A)	120.0(3)
C(2)–C(3)	1.531(3)	C(4B)–C(5)–C(6)	117.5(3)
C(3)–C(3A)	1.484(4)	C(3A)–C(9A)–C(1)	107.9(3)
C(3A)–C(9A)	1.342(4)	C(9)–C(9A)–C(1)	130.8(3)
C(4B)–C(5)	1.380(4)	C(5)–C(6)–C(7)	120.4(3)
C(4B)–C(8A)	1.400(4)	C(5)–C(6)–C(10)	119.6(3)
C(5)–C(6)	1.389(4)	C(7)–C(6)–C(10)	120.0(3)
C(6)–C(7)	1.396(4)	C(8)–C(7)–C(6)	120.6(3)
C(6)–C(10)	1.519(4)	O(3)–C(8)–C(7)	118.5(3)
C(7)–C(8)	1.370(4)	O(3)–C(8)–C(8A)	120.2(3)
C(8)–C(8A)	1.411(4)	C(7)–C(8)–C(8A)	121.3(3)
C(8A)–C(9)	1.452(4)	C(4B)–C(8A)–C(8)	115.9(3)
C(9)–C(9A)	1.437(4)	C(4B)–C(8A)–C(9)	122.4(3)
C(8)–O(3)–H(3)	104(2)	C(8)–C(8A)–C(9)	121.8(3)
C(3A)–O(4)–C(4B)	117.5(2)	O(2)–C(9)–C(9A)	124.8(3)
O(1)–C(1)–C(9A)	127.3(3)	O(2)–C(9)–C(8A)	122.2(3)
O(1)–C(1)–C(2)	125.1(3)	C(9A)–C(9)–C(8A)	113.0(3)
C(9A)–C(1)–C(2)	107.7(3)	C(3A)–C(9A)–C(9)	121.3(3)

Table 3. *Binding Parameters of Compounds* **1**, **2**, *and CPZ to* $(Ca^{+2})_4$-h*CaM Complex*

Compound	K_d(exp)[a]) [μM]	S[b])	K_i(theor)[c]) [μM]	EFEB[d]) [kcal/mol]
CPZ	1.24 ± 0.12	7.26 ± 0.38	3.87	−7.38
1	0.33 ± 0.11	4.50 ± 0.43	4.66	−7.27
2	0.76 ± 0.08	2.76 ± 0.27	5.26	−7.20

[a]) Experimental dissociation constant ± standard error. [b]) Binding stoichiometry ± standard error. [c]) Inhibition constant calculated with AutoDock 4. [d]) Estimated Free-Energy Binding.

In addition, the program predicts the possible site of interaction of the ligands into the protein. Docking of anthraquinones **1**, **2**, and CPZ into CaM (PDB code 1LIN) indicated that they bind in the same pocket. Gln8, Glu11, Phe12, and Met145 residues were involved in the interactions of CPZ (*Fig. 3*, *a*), while Gln8, Phe12, Ala73, and Lys75 participated in the binding of **1** and **2**; furthermore, Arg74 had one additional contact with compound **1** (*Fig. 3*, *b*). H-Bond was observed between Gln8 and the C(10)=O group of the anthraquinone moiety. As observed in *Table 3*, AutoDock predicted that the affinity of the antraquinones by CaM were similar to those of CPZ. Although the theoretical affinities of **1**, **2**, and CPZ were similar, the experimental data clearly revealed that **1** and **2** showed the smaller K_d values, and, in turn, higher affinity to CaM.

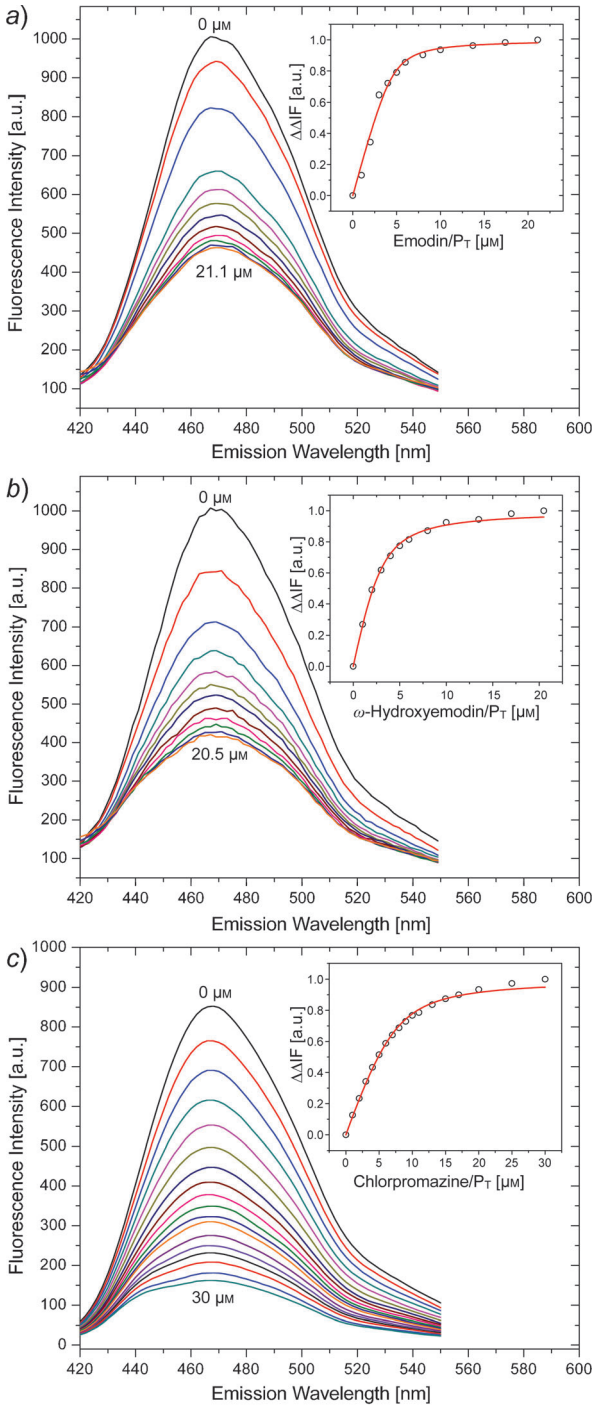

Fig. 2. *Titration curves of* h*CaM M124C*-mBBr *with* a) *emodin* (**1**), b) *ω-hydroxyemodin* (**2**), c) *CPZ, and* d) *citrinin* (**3**), *at saturation concentration of calcium ion* (10 μM of $CaCl_2$). The absolute changes of maximal fluorescence emission were plotted against the ratio ligands/protein total and fitted to a nonlinear equation (binding model) to obtain the K_d and stoichiometric ratio.

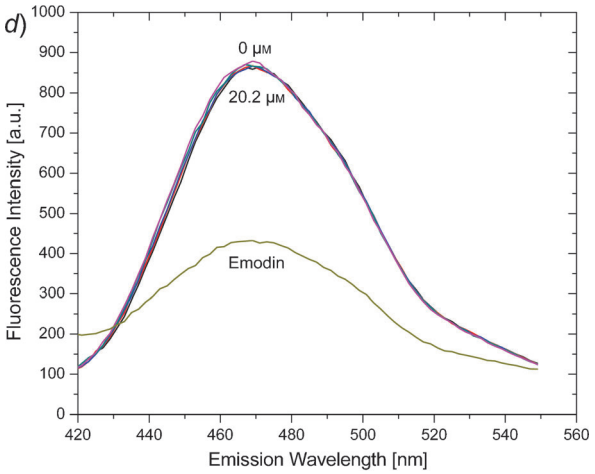

Fig. 2 (cont.)

The results presented demonstrated *in vitro* and *in silico* that **1** and **2** bind to CaM; this activity might be related with their biological properties. Thus, a number of studies have demonstrated that emodin (**1**) inhibited the growth and proliferation of various cancer cells by several mechanisms including inhibition of cell-cycle progression, apoptosis, reactive-oxygen-species generation, mitogen-activated protein kinases (MAPKs), and certain key enzymes and transcription factor, such as HER-2/neu, CKII, PKC, and NF-κB. In addition, *in vivo* studies have shown that **1** interrupted the progression of tumor metastasis through multiple signaling pathways. This strongly suggests that emodin (**1**) could be a promising candidate for the research and development of new antitumor drugs [23–25]. Finally, it is noteworthy that level of affinity of **1** to CaM is consistent with its ability to inhibit the activation of CaM-dependent cyclic nucleotide phosphodiesterase (PDE-1) [26].

Compound **2** has exhibited anti-inflammatory properties in bone-marrow mast cells due to attenuation of degranulation and 5-lipooxigenase-dependent leukotriene C_4 generation. In turn, the synthesis of leukotriene C_4 involves the activation of multiple-step signaling including MAP kinases activation by PKC, among others. Since it has been demonstrated that CaM is the key molecule for the activation of MAPK, it is highly probably that the anti-inflammatory properties of compound **2** are mediated by CaM. The finding that W-13, a potent inhibitor of CaM, inhibited MAPK activation provided additional evidence for this proposal [27–30].

This work was supported by grants from *DGAPA-UNAM* (IN218110) and *CONACyT 99395*. We thank *Georgina Duarte*, *Margarita Guzmán*, *Marisela Gutierrez*, *Isabel Rivero-Cruz*, *Araceli Pérez*, *Simón Hernández*, and *Hector Ríos* for their valuable technical assistance. The authors are very grateful to Dr. *A. Olson* and his colleagues at the *Scripps Research Institute* for providing AutoDock, and Dr. *S. Schooling*, Director PS&E, UCL Business PLC, for providing LigPlot software. *P. D. V.* acknowledges a fellowship from *CONACyT*. We are indebted to Dirección General de Cómputo y de Tecnologías de Información y Comunicación, UNAM, for providing the resources to carry out the computational calculations through the KanBalam supercomputing cluster.

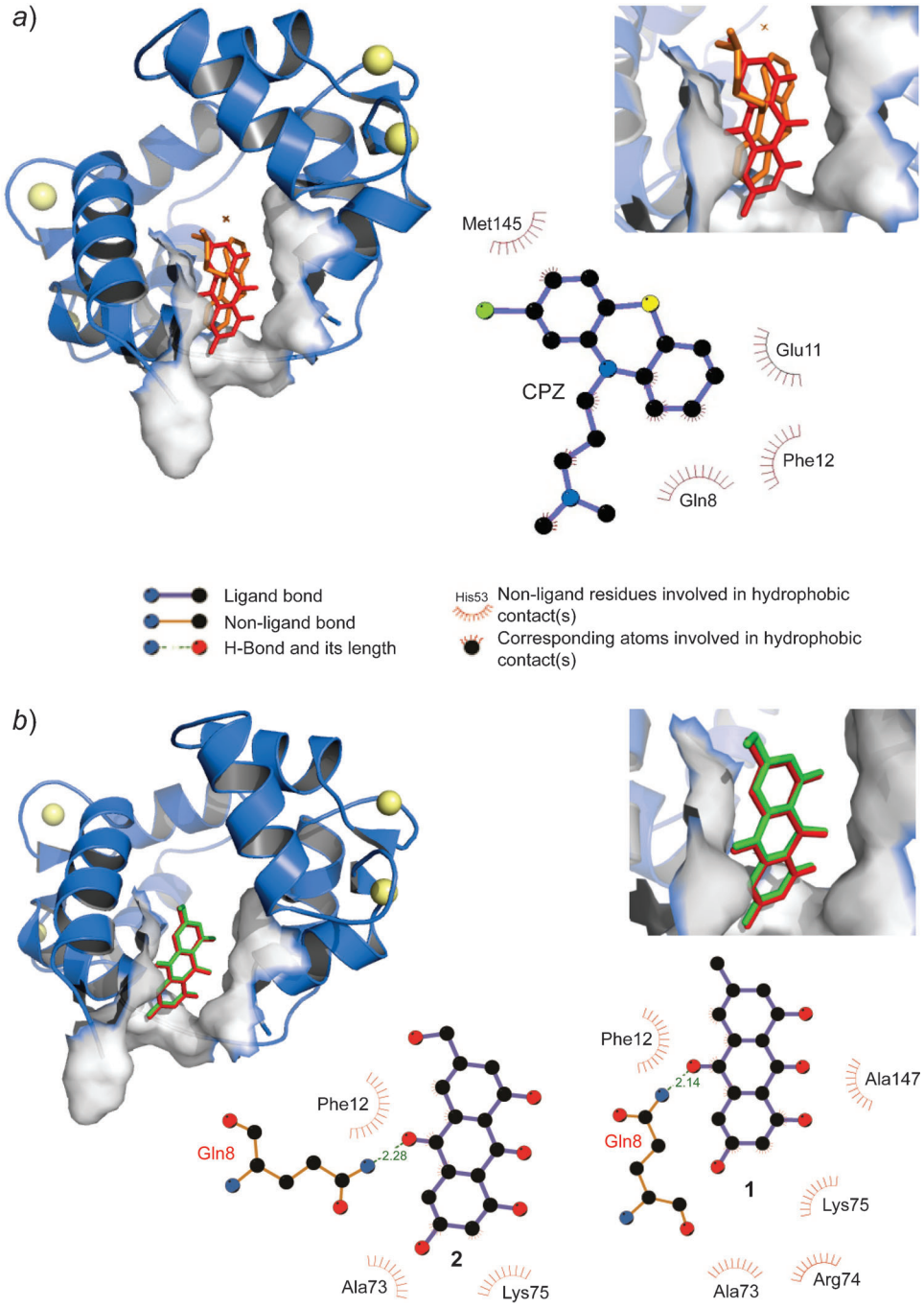

Fig. 3. *Structure model of* $(Ca^{+2})_4$-h*CaM with CPZ,* **1**, *and* **2**. *a*) CPZ and **1**; *b*) **1** and **2**. Shown in blue cartoon, orange stick, red stick, and green stick CaM, CPZ, **1** and **2**, respectively. The pocket of binding is shown in surface and denotes the 2D representation of $(Ca^{+2})_4$-*h*CaM–CPZ, $(Ca^{+2})_4$-*h*CaM–**1**, and $(Ca^{+2})_4$-*h*CaM–**2** interactions resulting from the docking. The images ware obtained with PyMOL and LigPlot.

Experimental Part

General. TLC: aluminum or glass plates coated with silica gel PF_{254} (*Merck*, D-Darmstadt). Open column chromatography (OCC): silica gel *60* (0.063–0.200 mm), 70–230 mesh (*Merck*), with a gradient system of hexane/CH_2Cl_2/MeOH, or *Sephadex® LH-20* with MeOH. M.p.: *Fisher–Johns* apparatus; uncorrected. UV Spectra: *Shimadzu 160* UV spectrophotometer at 25° in $CHCl_3$ soln. IR Spectra: in KBr on a *Perkin-Elmer 599B* spectrophotometer. ^{1}H-, ^{13}C-, and 2D-NMR spectra: *Varian Unity Inova* at 500 MHz (^{1}H)/125 MHz (^{13}C) in $CDCl_3$, CD_3OD, or $(CD_3)_2CO$, TMS as internal standard; chemical shifts as δ values in ppm. EI-MS: *JOEL JMS AX-505 HA* mass spectrometer; *m*/*z*.

Fungal Material. The culture of *Aspergillus stromatoides* was isolated from the sandy soil of Sánchez Magallanes beach located in the State of Tabasco in México (18° 17′ 46″ N, 93° 51′ 51″ W). The isolate of this fungus was maintained cryoconserved, and it was deposited with the mycological collection of the Herbario Nacional (MEXU), Instituto de Biología, Universidad Nacional Autónoma de México (voucher code MEXU 26344).

Fermentation, Extraction, and Isolation. One flask, containing the liquid potato-dextrose medium (10 l) was inoculated with 1 cm^2 agar plug taken from a potato-dextrose agar stock culture. The flask was cultured for 30 d at 30° under static conditions and in darkness. After the fermentation, the broth (10 l) was filtrated to give supernatant and mycelium. Next, the filtered growth medium was exhaustively extracted with CH_2Cl_2, and the resulting soln. was concentrated *in vacuo*. The mycelium was macerated with CH_2Cl_2 (3×2 l) during 8 d and filtered. The resulting org. soln. was dried (Na_2SO_4), and subsequently concentrated under reduced pressure. The org. extracts obtained from mycelium and culture medium were combined based on the chromatographic profiles to give a dark brown solid (5 g). From this extract crystallized **3** (160 mg). Four g of the org. extract were fractionated by OCC (silica-gel (200 g); gradient systems of hexane/CH_2Cl_2 and CH_2Cl_2/MeOH) to yield seven primary fractions, *Frs. 1–7*. All fractions were tested for their ability to quench the fluorescence of *h*CaM M124C-*mBBr*. Only *Fr. 6* at a concentration of 2 μg/ml quenched the fluorescence of the biosensor by *ca.* 55% (CPZ, at the concentration of 6 μM, quenched the fluorescence by 55%). The remaining fractions quenched the fluorescence of the biosensor less than 5%; therefore, they were considered inactive. Prep. TLC (CH_2Cl_2/MeOH 95:5) of active *Fr. 6* (eluted with CH_2Cl_2/MeOH 99:1) yielded compounds **1** (14 mg) and **2** (15 mg). From *Fr. 2*, eluted with hexane/CH_2Cl_2 6:4, crystallized spontaneously **4** (5 mg). *Fr. 4*, eluted with hexane/CH_2Cl_2 3:7, afforded 10 mg of **5**.

Emodine (=*1,3,8-Trihydroxy-6-methylanthracene-9,10-dione*; **1**). Orange needles. M.p. 254–255°. HR-EI-MS: 270.2417 (M^+, $C_{15}H_{10}O_5^+$; calc. 270.24).

ω-Hydroxyemodine (=*1,3,8-Trihydroxy-6-(hydroxymethyl)anthracene-9,10-dione*; **2**). Orange amorphous solid. M.p. 287–289°. HR-EI-MS: 286.0475 (M^+, $C_{15}H_{10}O_6^+$; calc. 286.23).

Citrinin (=*(3*R*,4*S*)-4,6-Dihydro-8-hydroxy-3,4,5-trimethyl-6-oxo-3*H*-2-benzopyran-7-carboxylic Acid*; **3**). Yellow crystals. M.p. 177–179°. HR-EI-MS: 250.0850 (M^+, $C_{15}H_{14}O_5^+$; calc. 250.24).

*Methyl 8-Hydroxy-6-methyl-9-oxo-9*H*-xanthene-1-carboxylate* (**4**). Pale-yellow crystals. M.p. 193°. HR-EI-MS: 284.0683 (M^+, $C_{16}H_{12}O_5^+$; calc. 284.26).

Coniochaetone A (=*2,3-Dihydro-8-hydroxy-6-methylbenzo[*b*]cyclopenta[*e*]pyran-1,9-dione*; **5**). Pale-orange crystals. M.p. 175–177°. HR-EI-MS: 230.0580 (M^+, $C_{13}H_{10}O_4^+$; calc. 230.21).

X-Ray Diffraction Analysis of **5**. A well-shaped prismatic single crystal of **5** was used for data collection on a *Bruker Smart APEX AXS* CCD diffractometer with graphite monochromator (MoK_α radiation). The final unit-cell parameters were based on all reflections. Data collection was performed with the Smart program [31]; integration and scaling of the reflections were carried out with the SAINT software [32]. The structure was solved with SIR2008 [33], and the models were refined by full-matrix least-square procedures on F^2 using SHELXL-97 [34]. Crystal data, data-collection procedures, structure-determination methods, and refinement results are collected in *Table 1*. Crystallographic data for the structure reported in this paper have been deposited with the *Cambridge Crystallographic Data Centre* (*CCDC*) as supplementary publication No. CCDC-899232. Copies of the data can be obtained, free of charge, from http://www.ccdc.cam.ac.uk/data_request/cif.

Steady-State Fluorescence. All measurements were conducted with an *ISS–PC1* spectrofluorometer (*ISS*, Champaign) with sample stirring at 37°. The protein *h*CaM M124C-*mBBr* (1 μM) was incubated in

buffer (10 mM of potassium acetate, pH 5.1) and $CaCl_2$ to saturation (10 μM). CPZ was used as positive control and citrinin (**3**) as a negative control. Fluorescence emission spectra were acquired with excitation and emission slit widths of 4 and 8 nm, resp. The excitation wavelength was 381 nm, and emissions at wavelengths of 415 to 550 nm were measured. The fractional degree of saturated *h*CaM M124C-*mBBr* with ligand (y) was calculated by changes in fluorescence on ligand binding according to $y=(F-F_0)/(F_\infty-F_0)$, where F_∞ represents the fluorescence intensity at saturation of the ligand, y is plotted as a function of the protein/ligand relation (L), and the apparent dissociation constants (K_d) and stoichiometry (S) were obtained by fitting to *Eqn. 1:*

$$y = \frac{(1 + K_d/S + L/S) - \sqrt{(1 + K_d/S + L/S)^2 - 4L/S}}{2} \quad (1)$$

where y represents the fractional degree of fluorescence intensity at 470 nm, K_d is the apparent dissociation constant for the ligands, L is the protein/ligand relation, and S is the stoichiometry. The data were analyzed using the Origin version 8.0 program (*OriginLab*, Northampton, MA).

Molecular Modelling. Docking was conducted using the PDB X-ray structure of CaM (PDB ID 1LIN.pdb). The crystal structures were rebuilt and refined after several interactions; finally, all-atom refinement of the protein was carried out using the idealization application of Rosetta v3.2 [35]. All compounds were built using the program HyperChem 8 and optimized geometrically using the program Gaussian 09, revision A.02 (*Gaussian Inc.*, Wallingford) at DTF B3LYP/3-21G level of theory. The protein and ligands were further prepared using the utilities implemented by AutoDockTools 1.5.4 (http://mgltools.scripps.edu/). Blind docking was carried out using AutoDock4 version 4.2 software (http://autodock.scripps.edu/) using the default parameters of the *Lamarkian* genetic algorithm with local search, number of individuals in population (150), maximum number of energy evaluations (2.5 million), maximum number of generations (27000), rate of gene mutation (0.02), rate of crossover (0.8), and 100 runs for docking. Electrostatic grid maps were generated for each atom type in the ligands using the auxiliary program AutoGrid4 part of the software AutoDock4. The initial grid box size was $60 \times 60 \times 60$ Å in the x, y, and z dimensions. To refine the initial docking results, the ligand was placed in a smaller grid box, with $30 \times 30 \times 30$ Å dimensions. The analysis of the docking was performed with AutoDockTools [20][21] using cluster analysis, LigPlot [22], and PyMOL [36]. All calculations were conducted using a parallel distributed memory supercomputer (Kanbalam, Dirección General de Cómputo y de Tecnologías de Información y Comunicación, UNAM) which contains 1368 processors AMD Opteron, *ca.* 3 terabyte of memory, and 160 terabyte of storage (http://www.super.unam.mx/).

REFERENCES

[1] D. Chin, A. R. Means, *Trends Cell Biol.* **2000**, *10*, 322.
[2] E. C. Seales, K. J. Micoli, J. M. McDonald, *J. Cell. Biochem.* **2006**, *97*, 45.
[3] J. Du, S. T. Szabo, N. A. Gray, H. K. Manji, *Int. J. Neuropsychopharmacol.* **2004**, *7*, 243.
[4] N. Mine, S. Yamamoto, N. Saito, S. Yamazaki, C. Suda, M. Ishigaki, D. W. Kufe, D. D. Von Hoff, T. Kawabe, *Mol. Cancer Ther.* **2011**, *10*, 1929.
[5] O. W. Rokhlin, A. F. Taghiyev, K. U. Bayer, D. Bumcrot, V. E. Koteliansk, R. A. Glover, M. B. Cohen, *Cancer Biol. Ther.* **2007**, *6*, 732.
[6] C. M. Coticchia, C. M. Revankar, T. B. Deb, R. B. Dickson, M. D. Johnson, *Breast Cancer Res. Treat.* **2009**, *115*, 545.
[7] J. Kjer, A. Debbab, A. H. Aly, P. Proksch, *Nat. Protoc.* **2010**, *5*, 479.
[8] M. González-Andrade, J. Rivera-Chávez, A. Sosa-Peinado, M. Figueroa, R. Rodríguez-Sotres, R. Mata, *J. Med. Chem.* **2011**, *54*, 3875.
[9] J. W. Bennett, 'An Overview of the Genus *Aspergillus*', in '*Aspergillus* Molecular Biology and Genomics', Eds. M. Machida, K. Gomi, Caister Academic Press, Norfolk, 2010, p. 1.

[10] S.-F. Li, Y.-T. Di, Y.-H. Wang, C.-J. Tan, X. Fang, Y. Zhang, Y.-T. Zheng, L. Li, H.-P. He, S.-L. Li, X.-J. Hao, *Helv. Chim. Acta* **2010**, *93*, 1795.
[11] H. Fujimoto, E. Nakamura, E. Okuyama, M. Ishibashi, *Chem. Pharm. Bull.* **2004**, *52*, 1005.
[12] A. M. R. Marinho, E. Rodrigues-Filho, *Helv. Chim. Acta* **2011**, *94*, 835.
[13] M. Macías, A. Gamboa, M. Ulloa, R. A. Toscano, R. Mata, *Phytochemistry* **2001**, *58*, 751.
[14] H.-J. Wang, J. B. Gloer, J. A. Scott, D. Malloch, *Tetrahedron Lett.* **1995**, *36*, 5847.
[15] M. González-Andrade, M. Figueroa, R. Rodríguez-Sotres, R. Mata, A. Sosa-Peinado, *Anal. Biochem.* **2009**, *387*, 64.
[16] T. Tanaka, T. Ohmura, H. Hidaka, *Mol. Pharmacol.* **1982**, *22*, 403.
[17] X. Lei, L. Zhang, B. Liu, *Yaoxue Xuebao* **1997**, *32*, 426.
[18] M. Golinski, P. J. DeLaLuz, R. Floresca, T. J. Delcamp, T. C. Vanaman, D. S. Watt, *Bioconjugate Chem.* **1995**, *6*, 549.
[19] M. Vandonselaar, R. A. Hickie, J. W. Quail, L. T. Delbaere, *Nat. Struct. Biol.* **1994**, *1*, 795.
[20] G. M. Morris, D. S. Goodsell, R. S. Halliday, R. Huey, W. E. Hart, R. K. Belew, A. J. Olson, *J. Comput. Chem.* **1998**, *19*, 1639.
[21] R. Huey, G. M. Morris, A. J. Olson, D. S. Goodsell, *J. Comput. Chem.* **2007**, *28*, 1145.
[22] A. C. Wallace, R. A. Laskowski, J. M. Thornton, *Protein Eng.* **1995**, *8*, 127.
[23] G. Srinivas, S. Babykutty, P. P. Sathiadevan, P. Srinivas, *Med. Res. Rev.* **2007**, *27*, 591.
[24] Q. Huang, G. Lu, H.-M. Shen, M. C. M. Chung, C. N. Ong, *Med. Res. Rev.* **2007**, *27*, 609.
[25] T. D. Palmer, W. J. Ashby, J. D. Lewis, A. Zijlstra, *Adv. Drug Delivery Rev.* **2011**, *63*, 568.
[26] R. Mata, A. Gamboa, M. Macías, S. Santillán, M. Ulloa, M. C. González, *J. Agric. Food Chem.* **2003**, *51*, 4559.
[27] Y. Lu, Y. Li, Y. Jahng, J.-K. Son, H. W. Chang, *Mol. Cell Biochem*. **2012**, *365*, 333.
[28] F. Tebar, A. LLadó, C. Enrich, *FEBS Lett*. **2002**, *517*, 206.
[29] F. Tebar, P. Villalonga, T. Sorkina, N. Agell, A. Sorkin, C. Enrich, *Mol. Biol. Cell* **2002**, *13*, 2057.
[30] T. Hirabayashi, T. Murayama, T. Shimizu, *Biol. Pharm. Bull.* **2004**, *27*, 1168.
[31] SMART (Version 5.625), *Bruker AXS Inc.*, Madison, 1999.
[32] SAINT (Version 6.23A), *Bruker AXS Inc.*, Madison, 1999.
[33] M. C. Burla, R. Caliandro, M. Camalli, B. Carrozzini, G. L. Cascarano, L. De Caro, C. Giacovazzo, G. Polidori, D. Siliqi, R. Spagna, *J. Appl. Crystallogr.* **2007**, *40*, 609.
[34] G. M. Sheldrick, SHELXL-97, Program for the Refinement of Crystal Structures, University of Göttingen, Göttingen, 1997.
[35] W. J. Wedemeyer, D. Baker, *Proteins* **2003**, *53*, 262.
[36] W. L. DeLano, The PyMol Molecular Graphic System, *DeLano Scientific*, San Carlos, 2002.

Received September 13, 2012